

A dusty X-ray absorber in the Perseus Cluster ?

K.A. Arnaud¹ & R.F. Mushotzky

Laboratory for High Energy Astrophysics, NASA/GSFC, Greenbelt MD 20771

ABSTRACT

We have analyzed 0.35–7.5 keV X-ray spectra of the center of the Perseus cluster collected using the Broad Band X-Ray Telescope (BBXRT) on the Astro-1 mission. These spectra are particularly useful for examining the nature of the X-ray absorber in cooling flows because of BBXRT’s sensitivity between 0.35 and 1.0 keV. We confirm that there is X-ray absorption above that expected from gas in our own galaxy. Further, the absorbing medium is deficient in helium. However, the energy of the K-edge of oxygen is consistent with neutral material (at the redshift of the cluster) and is not consistent with any ionized state of oxygen. It is not possible to completely ionize helium and have oxygen neutral so the apparent helium deficiency cannot be due to ionization. We propose that the X-ray absorption is due to dust grains that have condensed out of a medium in which helium remains ionized. This model satisfies all the observational constraints but is difficult to understand theoretically.

Subject headings: galaxies: clusters, cooling flows, X-rays: galaxies

1. Introduction

Clusters of galaxies are prodigious sources of X-ray emission, produced by a $10^7 - 10^8$ K plasma confined by the gravitational field of the cluster. In the inner tens of kpc of many clusters the radiative cooling time of this gas is less than the age of the cluster implying that the gas cannot be static and must be cooling and flowing into the center (see eg Fabian 1994 and references therein). This picture has been verified by both X-ray imaging and spectroscopy with the implied cooling rates being, in some cases, many hundreds of Solar masses per year.

This led to the central mystery of cooling flows : if so much mass is cooling through the X-ray band ($T \sim 10^7$ K) what happens to it after that ? Solutions can be roughly classified into three camps : a) the X-ray data analysis is wrong, b) there is energy input which prevents the gas cooling out of the X-ray regime, and c) the gas cools down and condenses into something that is not observed (eg low mass stars). Solution a) has been shown to be incorrect by the consistent results obtained using a variety of different detectors and analysis methods. Solution b)

¹also Astronomy Department, University of Maryland

is much argued over and seems to us to require an unlikely amount of fine tuning. Solution c) is unsatisfactory in that it posits placing the mass in something that cannot be seen. There is some evidence for star formation in the galaxies at the centers of cooling flows but with a conventional initial mass function this can mop up only 1–10% of the available mass (e.g. McNamara 1997).

Solution c) received a large boost following the observation by White et al. (1991) that cooling flows showed X-ray absorption in excess of that from our own Galaxy. The column densities observed were consistent with the accumulation of cooling flow matter over the lifetime of the cluster. These excess absorptions were confirmed by analysis of spectra obtained using ROSAT (Allen et al. 1993) and ASCA (Fabian et al. 1994). However, this cold, absorbing material is not seen in HI or CO (e.g. O’Dea & Baum 1997). Again, we obtain a result using X-ray data but cannot find the corollaries in other wavebands. A further problem is that the excess absorption does not always show up in the analysis of spectra obtained using the ROSAT PSPC (e.g. Sarazin 1997). Since the ROSAT PSPC has a lower energy cut-off than ASCA it should provide a more sensitive measurement of absorption.

In this paper we report investigations on the nature of the X-ray absorber in the Perseus cluster, a much-studied, massive cooling flow centered on the galaxy NGC 1275. We use data from the Broad Band X-Ray Telescope (BBXRT) that flew on the Astro-1 Space Shuttle mission December 2–10, 1990. BBXRT used telescopes similar to those on ASCA but with segmented Si(Li) solid-state detectors instead of CCDs. The BBXRT Si(Li) detectors have slightly lower spectral resolution than the ASCA CCDs but they do not have the instrumental oxygen absorption which reduces the CCDs’ efficiency immediately above 0.5 keV. Since the primary absorption feature in the energy range covered by these detectors is the O K edge, BBXRT data provide a more sensitive measurement of the redshift and detailed shape of the X-ray absorption than is possible with ASCA.

2. Instrument and Observation Description

BBXRT (Serlemitsos et al. 1991, Petre et al. 1991, Weaver et al. 1995) was flown on the Space Shuttle Columbia (STS-35) as part of the nine day Astro-1 mission (Blair & Gull 1990). BBXRT consisted of two grazing-incidence conical foil telescopes with focal lengths of 3.8m. These telescopes had a spatial resolution whose integral power can be characterized by two error functions : 65% of the reflected photons are distributed with an half-power diameter (HPD) of 1.3 arcminutes and the rest with an HPD of 5.8 arcminutes. The system was sensitive to X-rays with energies up to 12 keV, an upper limit determined by the focal length, although the effective area dropped off rapidly as this energy was approached since there were few foils available to focus X-rays requiring such small grazing angles. The mirrors were prototypes for those used on ASCA and have similar properties.

The focal plane instrumentation consisted of two segmented Si(Li) solid-state detectors.

Each detector was divided into five independent pixels, a central 4 arcmin diameter pixel and four outer quadrant pixels covering a total diameter of 17 arcmin with 1 arcmin gaps between individual pixels. We refer to the central detector segments as A0 and B0 with the A system being that for the telescope whose axis is taken as the nominal pointing direction. The telescopes were misaligned by $\sim 1'$. The outer quadrant pixels for the A system are labelled A1 – A4 in an anticlockwise direction on the sky with the roll angle defined by the angle between due East and the A1/A2 dividing line. The B outer pixels are rotated by 180 degrees with respect to the A system so B1 corresponds to A3, B2 to A4 etc. The central pixels had an energy resolution of $\sim 165\text{eV}$ (FWHM) at 6 keV and the outer pixels a resolution of $\sim 190\text{eV}$. Each detector returned spectra in 512 channels, the first 256 being approximately 16 eV wide and the rest 32 eV wide. Background rejection was performed using a combination of criteria, the most important of which were pixel-pixel coincidence and the triggering of a wrap-around plastic scintillator.

BBXRT pointed in the direction of the Perseus cluster on four occasions during the Astro-1 mission (there were several more very brief observations). The observation analyzed here was the longest and highest signal-to-noise. It occurred on day 6 of the mission. Star-tracker data shows that the pointing position was $\alpha = 49.12$, $\delta = 41.38$, approximately 3 arcminutes from NGC 1275. This placed the center of the cluster on a gap between pixels. The roll angle was 120 degrees so the cooling flow region was distributed between pixels A0 and A3 on one telescope and B0 and B1 on the other. The exposure time was 2542.5 seconds. The observation on day 3 was also pointed at the center of the cluster however its exposure time of 330 seconds is too short to provide useful data.

We used the source spectra, background spectra, and response matrices from the HEASARC archive. These were generated using the standard procedures given in Weaver et al. (1995). We note, in particular, that this observation occurred during orbit night so there is no danger of contamination due to an atmospheric oxygen line.

In our analysis we used channels starting at 0.35 keV for A0 and B0, 0.44 keV for A3 and 0.60 keV for B1. The outer pixels were less reliable at very low energies, and those on the B telescope particularly so (Weaver et al. 1995). We cut off all the spectra at 7.5 keV because of the sharp decrease in telescope effective area above this energy. We grouped the spectra so that each bin contained at least 20 counts (although this only affected the extreme high energy end). We subtracted background although the effect is negligible.

In our analysis we fitted models to all four spectra simultaneously but left their relative normalizations as free parameters.

3. Results of fits to the data

We started by fitting a simple series of models to the data in order to test if we were in agreement with the results from the ASCA SIS published by Fabian et al. (1994). We used XSPEC

v10 (Arnaud 1996) to fit the following series of models to the data. First, a single temperature Raymond-Smith plasma (RS: Raymond & Smith 1977) with photoelectric absorption from the Galactic column ($1.37 \times 10^{21} \text{ cm}^{-2}$: Stark et al. 1992). The data (for pixel A0 only) and this model are shown in Figure 1. The deficit of model flux between 1 and 2 keV indicates that an additional lower temperature component is required. However, the model lies above the data between 0.5 and 1 keV so extra absorption is also necessary. We added a second component with its own absorption, assumed to be at the redshift of the cluster ($z = 0.0183$). This second component was, successively, another single temperature RS plasma, a cooling flow model consisting of emission from a range of temperatures (Mushotzky & Szymkowiak 1988), and a cooling flow model using the Mewe-Kaastra-Liedahl plasma model (MK: Mewe, Gronenschild & van den Oord 1985; Mewe, Lemen & van den Oord 1986; Kaastra 1992, Liedahl, Osterheld & Goldstein 1995). The results are shown in table 1. None of the models provides a good fit to the BBXRT data (as was true with the ASCA data). The fit parameters are in broad agreement between the two sets of detectors. The amount of extra absorption required is the largest difference between the BBXRT and ASCA results. This parameter is determined by precisely the energy range where the BBXRT and ASCA sensitivities differ the most.

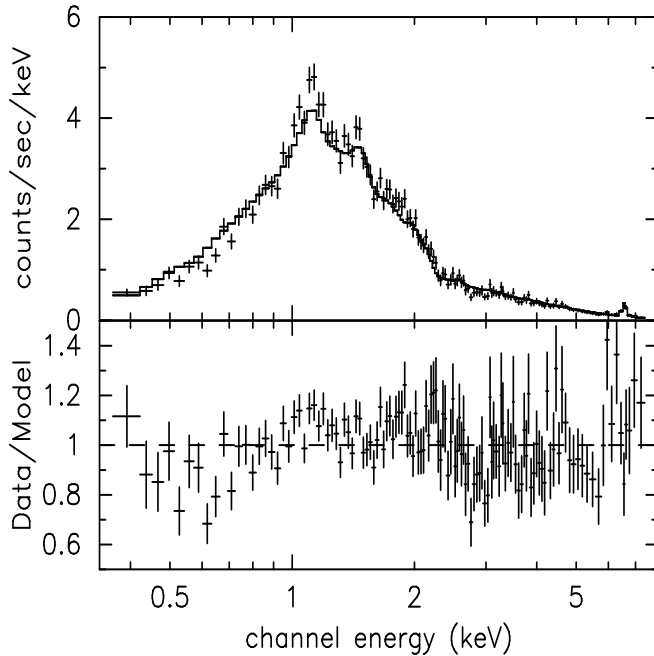


Figure 1. The upper panel shows the A0 data (crosses) and model (stepped line) for the single temperature fit. The lower panel shows the data divided by the model. The vertical bars on the data are one sigma errors.

The strongest absorption feature in the energy range covered by the BBXRT data is due to the oxygen K edge. So, we replaced the redshifted absorption with an edge and found its best-fit energy and confidence range. The result for the model using the RS cooling flow is shown in Figure 2. We have checked the channel-energy relation by fitting an oxygen fluorescence line to BBXRT bright Earth data. We find an energy of $528 \pm 1\text{eV}$, which is 3eV above the theoretical value. The bands marked $z=0$ and $z=0.0183$ on Figure 2 are the edge energies shifted by 3eV to

correct for this slight miscalibration ².

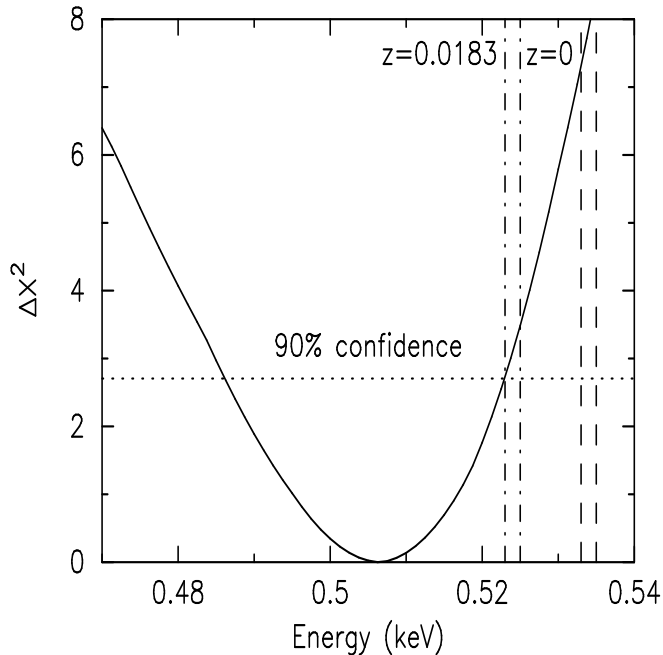


Figure 2. The confidence region for the edge energy from fitting an RS cooling flow model and edge to the BBXRT data. The horizontal dotted line is at $\Delta\chi^2 = 2.71$, corresponding to 90% confidence on one interesting parameter. The vertical bands are edge energies (with calibration uncertainties) for an absorber at the redshift of the cluster and at zero redshift.

The widths of the bands reflect the uncertainty in the gain calibration. Formally, we can rule out at $>90\%$ confidence the oxygen edge being due to material in the Galaxy. However, there are 5-10% uncertainties in the effective area calibration in this energy range (Weaver et al. 1995) which must affect the measurement of the edge energy. So, a conservative statement would be that the edge energy is better fit by an absorber in the rest frame of the cluster but we cannot rule out a zero redshift absorber. The K edge of singly-ionized oxygen is ~ 20 eV above that for neutral material. An edge at this energy is ruled out by the BBXRT data so the oxygen in the absorbing material must be neutral.

The model with a single oxygen edge is a significantly better fit to the data than that with

²There is some dispute about the energy of the oxygen K edge. The value used in the photoelectric absorption routines commonly used in X-ray astronomy (e.g. Balucinska-Church & McCammon 1994) is 532 eV. However, Schattenburg & Canizares (1986) place a lower limit on the edge energy of ~ 536 eV using FPCS observations of the Crab nebula. These authors note that a possible explanation for the discrepancy is that the 532 eV value given in the literature is the energy required to promote a K-shell electron to the Fermi level, rather than to the continuum. This could produce a ~ 5 eV shift. Indeed, Verner et al. (1996) place the edge at 537 eV. However, Gould & Jung (1991) argue that the current experimental measurements are not relevant to the astrophysical context and their theoretical calculation gives an edge energy of 546 eV. The latest results from the Opacity Project give an edge energy of 549 eV (Pradhan & Zhang, priv.comm.) We calibrated the gain of BBXRT assuming a fluorescent line energy of 525 eV. This corresponds to an edge at 537 eV. If the edge is at a higher energy then so is the fluorescence line and our gain calibration is changed. Thus any result on the redshift of the edge is independent of the actual correct edge energy. We did modify the Balucinska-Church & McCammon (1994) subroutine to use 537 eV. We also tested our results using the cross-sections of Verner et al. (1996) and found no significant changes.

standard photoelectric absorption. For the RS cooling flow model the former gives $\chi^2=1185$ and the latter $\chi^2=1211$. We will refer to these two models as the “edge” and “absorption” models respectively. The difference between the fits is illustrated in Figure 3, which shows the ratios of data to best-fit model for the two cases. The “absorption” model leads to a systematic slope to the residuals between 0.4 and 0.6 keV while the “edge” model gives flat residuals in this energy range.

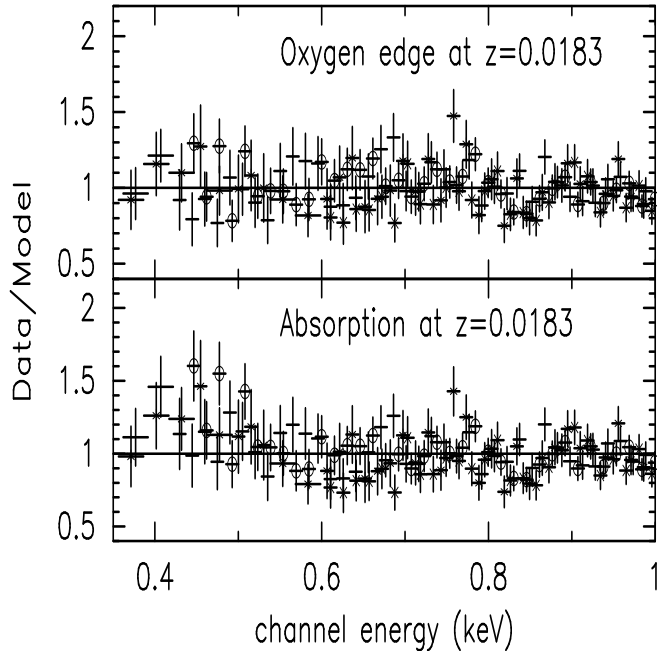


Figure 3. The upper panel shows the ratio of data to best-fit model for a single edge modifying the cooling flow while the lower panel is for a standard photoelectric absorption model modifying the cooling flow. The four detector pixels are indicated by different symbols.

We have checked that the slope in the “absorption” model residuals cannot be due to systematic problems in the instrument calibration by looking at the BBXRT observations of the Crab nebula (see also Weaver et al. 1995). We have compared the ratios of central pixel (A0 and B0) data to best-fit model for the Perseus and Crab nebula observations. Figure 4 shows the ratio of data to absorbed power-law model for the Crab (circle symbols) and the ratio of data to “absorption” model for the Perseus cluster. The Perseus cluster residuals differ systematically from those for the Crab nebula so the “absorption” model residuals cannot be due to a calibration problem.

In our attempts to find a good model for the data including standard photoelectric absorption we have tried changing from a RS-based cooling flow to one based on MK. We have also tried varying the assumed minimum temperature of the flow and the slope of the differential emission measure function (Mushotzky & Szymkowiak 1988). None of these changes improve the fit below 0.7 keV. The reason why none of these changes work can be seen in Figure 5. This figure shows the “absorption” model used to give the residuals in the lower panel of Figure 3. The lower line is the cooling flow component modified by its absorption, the middle line is the single temperature RS model, and the top line is the sum of the two. The cooling flow component does not contribute

significantly to the model below about 0.7 keV. Hence, modifying this component cannot improve the fit in the 0.4–0.6 keV range.

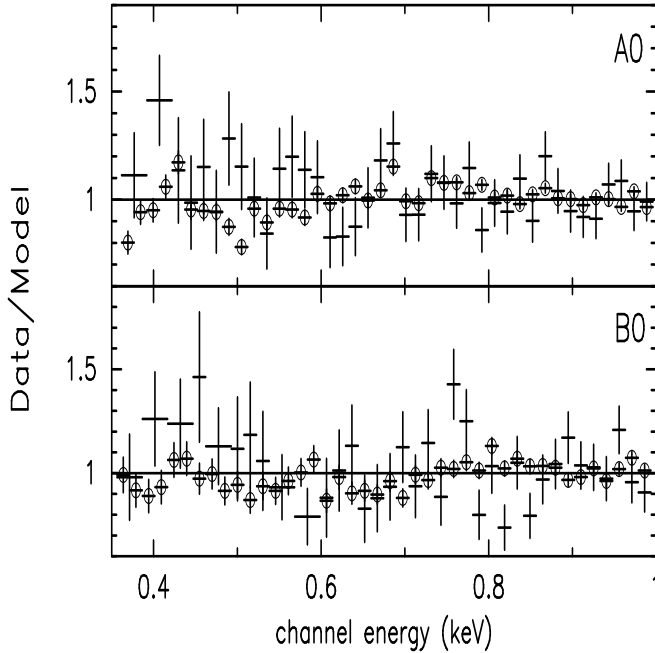


Figure 4. The points indicated by circle symbols and with smaller error bars are the ratio of the data to best-fit power-law model for the Crab nebula. The other points are the ratio of the Perseus cluster data to the cooling flow modified by the standard photoelectric absorption model (ie the lower panel in Figure 3). The upper panel is for detector pixel A0 and the lower for B0. Note that the Perseus cluster points are systematically high relative to the Crab points for energies between 0.4 and 0.6 keV.

We also note that although the 2-temperature model with absorption gives a lower total χ^2 than the cooling flow with an edge the residuals below 0.7 keV still show the systematic problem. Indeed, a 2-temperature model with an edge gives $\chi^2=1166$, the lowest of any model we tried.

The “absorption” model used above assumes that the cooling flow region is in the center of the cluster, outside that there is a skin of cold absorbing material, and outside that the ambient medium, represented by the single temperature RS model. This is physically implausible. There are a large number of ways that the absorbing medium can be distributed; we have looked at two representative examples. Firstly, we suppose that some fraction of the cooling flow is outside the absorbing material and the rest is inside. This can be described by a partial covering fraction model. Attempting to fit this model to the data gave a best fit with unit covering fraction. Alternatively, we supposed that the absorbing clouds are distributed uniformly throughout the cooling flow region. Allen & Fabian (1997) called this the multilayer absorber model. It has a transmission given by $(1 - e^{-\sigma(E)N_H})/(\sigma(E)N_H)$, where $\sigma(E)$ is the absorption cross-section and N_H is the total column through the cooling flow region. We fit this model to the data and found that it did even worse than the simple absorption model ($\chi^2=1229$ vs. $\chi^2=1211$) and did not solve the problem at low energies.

Figure 6 illustrates why these modifications to the “absorption” model do not work. The solid curve is the “absorption” model and the dashed curve is “edge” model. Almost the only difference is that the “edge” model gives more flux in the range 0.4–0.5 keV. The modified absorption models

do allow more flux through in this energy range but at the expense of flattening the spectrum in the range 0.5–1.0 keV, which the data do not allow.

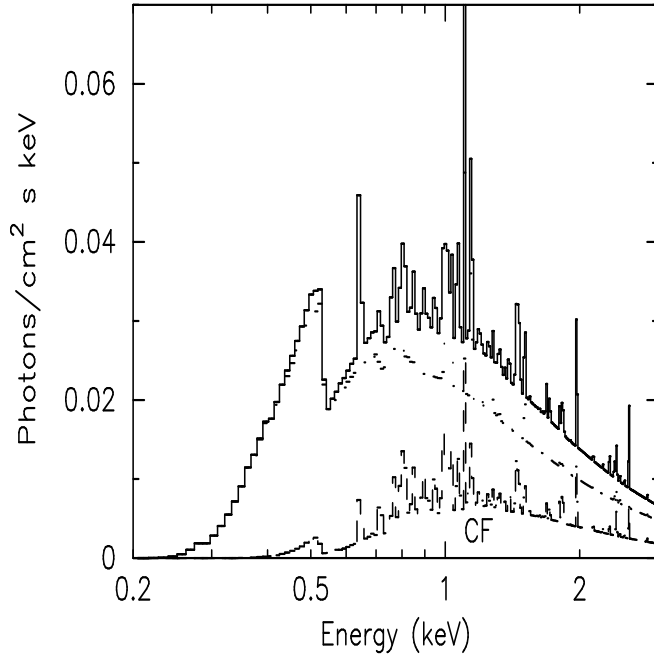


Figure 5. The theoretical model components for the photoelectric absorption case shown in the lower panel of figure 3. The lower (dashed - labelled CF) line is the cooling flow component modified by its absorption, the middle (dashed) line is the single temperature RS model, and the top (full) line is the sum of the two.

The only option left is to change the relative abundances of elements in the absorber. To get an idea of which abundances mattered the most we first set the abundances of all elements other than O to zero. Then we set each element in turn to Solar abundance (Anders & Grevesse 1989) relative to O and fit for the other free parameters. The elements that produced the greatest increase in χ^2 were Ne, He, H, C, Mg, Fe with $\Delta\chi^2$ of +15, +14, +6, +6, +5, +5 respectively. The Ne K-edge is at ~ 0.87 keV, in the energy range where the cooling flow makes a significant contribution. In view of this and the systematic differences between the data and the model in this energy range visible in figure 3, we prefer not to draw strong conclusions from the lack of Ne absorption. However, there are no systematic problems below the O K-edge, where absorption is dominated by He. Consequently, we consider the He result to be firm. Thus the data imply a large deficiency in He abundance with respect to O. We then assumed that H, He, and Ne have their standard relative abundances and then fit for their abundance relative to oxygen. We found that the combination of H, He, and Ne must be underabundant relative to O by a factor of 10 with respect to Solar abundances. We performed a similar test for C and found that it must be underabundant relative to O by a factor of 3.

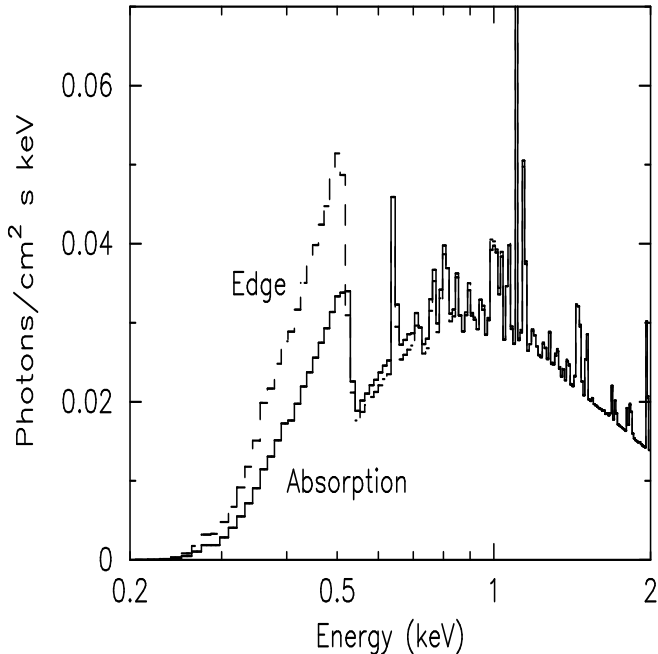


Figure 6. The two theoretical models used in figure 3 plotted on the same graph. The solid line is for standard photoelectric absorption and the dashed line is for the single edge.

4. Discussion

The simplest way to produce O absorption without He absorption is to suppose that the He is completely ionized. However, the O K-edge seen in the BBXRT spectrum is from neutral material. We can rule out even singly-ionized oxygen, whose K-edge is ~ 20 eV higher than that of neutral oxygen. It is not possible to have both neutral O and completely ionized He either for collisional (e.g. Arnaud & Rothenflug 1985) or photoionized (e.g. Kallman & McCray 1982) equilibrium plasmas. So, we can rule out ionization as a mechanism for the deficit in absorption due to He.

The argument in the previous paragraph holds only if the He and O are mixed together in the gaseous state. One way to combine neutral O and ionized He is to suppose that the O is in grains that have condensed out of the gas. This explanation is bolstered by the result on Ne absorption. He and Ne are noble gases and are not depleted onto grains.

It would be overinterpreting data of this signal-to-noise and resolution to attempt to deduce abundance ratios in the grains. We merely comment that we do not expect the absorber to have Solar abundance ratios. Mushotzky et al. (1996) show that the relative abundances in the intracluster medium of O, Ne, Mg, Si, S, and Fe are non-Solar and are consistent with production in Type II supernovae. There are no observations giving the abundance of C in intracluster gas. Since C is not a Type II supernova product we might expect it to be underabundant with respect to O.

An He deficiency provides a possible explanation for discrepancies found between measurements

using the ROSAT PSPC and measurements using other detectors. The determination of an absorption column using the PSPC is dominated by data in the energy range 0.2–0.5 keV (see for instance figure 1 in Sarazin 1997). The absorption in this energy range is mainly due to He. Since the cooling flow absorber in the Perseus cluster is apparently deficient in this element the PSPC will be insensitive to the extra absorption and will tend to measure only the Galactic absorption column. The significant extra absorption in the Perseus cluster measured by Allen & Fabian (1997) was based on PSPC 0.41–2.00 keV data. In this energy range using the PSPC oxygen is the dominant absorber so extra absorption is detected. Allen & Fabian (1997) do consider energies down to 0.2 keV for the spectra from A1795 and A2199. Using these data they find smaller excess columns than if they used spectra starting at 0.4 keV. We interpret this as evidence for a He deficiency in the absorber in these two clusters. Allen & Fabian (1997) did not use the low energy data in general because the ROSAT PSPC spatial resolution is worse than at higher energies and they were interested in the spatial distribution of the absorber. We have analyzed the entire ROSAT PSPC spectrum of the whole cooling flow region in Perseus (which is large enough that we don't have to worry about the energy-dependent spatial resolution). For a wide variety of emission models we find that the absorption is consistent with the Galactic column. Although there are problems with the calibration of the ROSAT PSPC (Snowden priv. comm.) these do not affect the measurement of the absorption column. This provides confirmatory evidence for absorber He deficiency found using the BBXRT data. The poor spectral resolution and large instrumental carbon edge make the sort of analysis performed in this paper extremely difficult using the PSPC.

The presence of dust around NGC 1275 has been deduced from dark regions in optical images (McNamara, O'Connell & Sarazin 1996), the ratios of emission lines in the optical filaments (Hu 1992; Donahue & Voit 1993), and far-IR emission (Lester et al. 1995). The observed X-ray absorption column and cooling flow luminosity require the grains to absorb about 5×10^{43} erg/s (we use $H_0 = 50$ km/s/Mpc throughout). The exact absorbed luminosity depends on the distribution of absorption and emission in the BBXRT field-of-view. The 40–120 μ m luminosity quoted by Lester et al. (1995) is double this absorbed X-ray luminosity. So the absorbed X-ray energy could be reradiated in the far-IR.

The O column deduced from the X-ray absorption is $\sim 2 \times 10^{18}$ atoms/cm². If the absorber is associated with the cooling flow and is distributed across the cooling region this gives a mass in O of $\sim 4 \times 10^9 f M_\odot$, where f is the covering fraction of the cooling flow and absorption. For $f \sim 1$ this is a mass in grains two orders of magnitude larger than that deduced from the far-IR emission (Jura et al. 1987; Lester et al. 1995). However, the far-IR emission is not distributed across the cooling flow but appears to correlate with the emission line filaments (Lester et al. 1995). We are led to one of two conclusions: a) the cooling flow emission and its absorbing dust cover $\sim 1\%$ of the cooling region and correlate with the emission line filaments, or b) the cooling flow emission and absorbing dust are distributed across the cooling region but outside the emission line filaments the dust is too cold to radiate significantly at 100 μ m (ie $T \lesssim 10$ K). Option a) is ruled out by the high spatial resolution X-ray observations which do not show any correlation between X-ray emission

and emission line filaments (Böhringer et al. 1993; McNamara, O’Connell & Sarazin 1996).

We emphasise that it is the lack of correlation between the X-ray emission and the optical filaments that it is critical. If the X-ray emission and absorption from the cooling flow had been associated with the filaments then we could have built a coherent picture involving absorption due to the warm dust and molecules which are seen (Lester et al. 1995; Lazareff et al. 1989; Mirabel et al. 1989). We can reduce the mass in dust required by supposing that the cooling flow and its absorber are distributed throughout the cooling region but are inhomogeneous on a scale smaller than the resolution of the ROSAT HRI. There is no observational data on the covering fraction at these spatial resolutions. There is evidence in the Centaurus clusters for a volume filling factor less than one. Fukazawa et al. (1994) showed that in the cooling region the lower temperature component occupied a volume one twentieth of that of the hotter ambient medium. The relation between the volume filling factor and the covering fraction will depend on the details of the cooling flow.

The identification of the X-ray absorber with cold dust explains all the observations but poses severe theoretical problems. Dust should be destroyed by sputtering in the central regions of the cluster (Dwek & Arendt 1992). Some of the dust could be in the outer parts of the cluster (e.g. Hu 1992) however Allen & Fabian (1997) show that the excess absorption is concentrated in the core of the cluster, within the cooling region. So, we require that cold ($\lesssim 10\text{K}$) dust co-exist in the cooling region with gas of densities $> 10^{-2}\text{cm}^{-2}$ and temperatures of $\sim 10^7$ K. Further, if the dust is formed from the cooling flow then the gas needs to cool below the condensation temperature (~ 2000 K) but be ionized such that He is completely stripped. The optical spectrum of the stars in NGC 1275 is not reddened above that expected due to dust in our own galaxy. This requires that the dust grains be large enough to be opaque. Since the timescale for dust destruction by sputtering is proportional to grain size, the smaller grains, which provide the optical reddening, will not survive.

Dust appears to form easily whenever the gas temperature drops below the condensation temperature for grains (e.g. SN1987A: Colgan et al. 1994) and in AGN grains co-exist with ionized gas (e.g. Brandt, Fabian & Pounds 1996). Fabian, Johnstone & Daines (1994) argued that cold, dusty clouds can form in cooling flows. However, these clouds will also contain cold He so will absorb X-rays below the neutral O K-edge. Voit & Donahue (1995) pointed out that CO would be evaporated off grains by transient X-ray heating from the cluster gas. In this case most of the oxygen would not be on grains but in molecular gas whose luminosity would exceed that observed in the CO rotational lines. Also, heating of the grains by collisions with hot electrons from the cluster gas is capable of supplying more than enough energy to surpass the far-IR luminosity observed (Lester et al. 1995). We have no solution to these problems.

We note in passing that Czerny et al. (1995) considered X-ray absorption by dust grains in AGN. They showed that if dust rather than gas is the absorbing medium then more flux will be detected around 0.4 keV and this may explain some observations of soft excesses above a

power-law spectrum absorbed by gas.

5. Conclusions

We have shown that the BBXRT spectra of the Perseus Cluster are consistent with a cooling flow absorber at the redshift of the cluster. The data are marginally inconsistent with the absorber being local to our galaxy. More important, we have demonstrated that the absorber is deficient in helium (and, with less confidence, neon). The only reasonable explanation of this is that the absorber is comprised of dust grains formed out of gas in which helium is completely ionized. The absorption model we have fit assumes that the dust grains are a screen in front of the cooling flow. This is oversimplistic and it is likely that they are distributed throughout the cooling flow. The present data are not good enough to explore this issue.

A model in which cold grains are distributed throughout the cooling region and are heated only where there are emission line filaments satisfies all the observational constraints. However, we do not understand how to keep the oxygen on the grains, how to prevent the grains being destroyed, or how to keep the grains at very low effective temperatures.

BBXRT also observed the cooling flow clusters Abell 262 and Abell 496. These data are not as high quality as those for Perseus and all we can conclude for these clusters is that there is an O K edge present whose depth exceeds that expected from the Galactic column (Mackenzie, Schlegel & Mushotzky 1996).

Our result could be confirmed using the the backside-illuminated ACIS CCDs on AXAF. In the future, high resolution spectroscopy will provide detailed information about abundances, ionization states, and grain composition from the energies, depths, and detailed shapes of absorption edges (see e.g. Woo, Forrey & Cho 1997).

We thank Ari Laor for reminding us that we had never published this data. We thank Hagai Netzer and Tim Kallman for helpful discussions. This research has made use of data obtained through the High Energy Astrophysics Science Archive Research Center Online Service, provided by the NASA/Goddard Space Flight Center.

REFERENCES

- Allen, S.W., Fabian, A.C., Johnstone, R.M., White, D.A., Daines, S.J., Edge, A.C. & Stewart, G.C., 1993, MNRAS, 262, 901
- Allen, S.W. & Fabian, A.C., 1997, MNRAS, 286, 583
- Anders, E. & Grevesse, N., 1989, *Geochemica et Cosmochimica Acta*, 53, 197
- Arnaud, K.A., 1996, in *Astronomical Data Analysis Software and Systems V*, eds. Jacoby G. & Barnes J., ASP Conf. Series
- Arnaud, M. & Rothenflug R., 1985, A&AS, 60, 425
- Balucinska-Church, M. & McCammon, D., 1992, ApJ, 400, 699
- Blair, W.P. & Gull, T.R., 1990, S&T, 79, 591
- Böhringer, H., Voges, W., Fabian, A.C., Edge, A.C., Neumann, D.M., 1993, MNRAS, 264, L25
- Brandt, W.N., Fabian, A.C. & Pounds, K.A., 1996, MNRAS, 278, 326
- Colgan, S.W.J., Haas, M.R., Erickson, E.F., Lord, S.D., Hollenbach, D.J., 1994, ApJ, 427, 874
- Czerny, B., Loska, Z., Szczerba, R., Cukierska, J. & Madejski, G., 1995, *Acta Astronomica*, 45, 623
- Donahue, M. & Voit, G.M., 1993, ApJ, 414, L17
- Dwek, E. & Arendt, R.G, 1992, ARA&A, 30, 11
- Fabian, A.C., 1994, ARA&A, 32, 227
- Fabian, A.C., Arnaud, K.A., Bautz, M.W. & Tawara, Y., 1994, ApJ, 436, L63
- Fabian, A.C., Johnstone, R.M. & Daines, S.J., 1994, MNRAS, 271, 737
- Fukazawa, Y., Ohashi, T., Fabian, A.C., Canizares, C.R., Ikebe, Y., Makishima, K., Mushotzky, R.F. & Yamashita, K., 1994, PASJ, 46, L55
- Gould, R., & Jung, Y-D., 1991, ApJ, 373, 271
- Hu, E., 1992, ApJ, 391, 608
- Jura, M., Kim, D.-W., Knapp, G.R. & Guhathakurta, P., 1987, ApJ, 312, L11
- Kaastra, J.S., 1992. Internal SRON-Leiden report, version 2.0
- Kallman, T.R. & McCray, R., 1982, ApJS, 50, 263
- Lazareff, B., Castets, A., Kim, D.-W. & Jura, M., 1989, ApJ, 336, L13
- Liedahl, D.A., Osterheld, A.L. & Goldstein, W.H., 1995, ApJ, 438, L115
- Lester, D.F., Zink, E.C., Doppmann, G.W., Gaffney, N.I., Harvey, P.M., Smith, B.J. & Malkan, M., 1995, ApJ, 439, 185
- Makenzie, M., Schlegel, E.M. & Mushotzky, R.F., 1996, ApJ, 468, 86

- McNamara, B.R., O’Connell, R.W. & Sarazin, C.L., 1996, *AJ*, 112, 91
- McNamara, B.R., 1997, in *Galactic and Cluster Cooling Flows*, ed. N. Soker, ASP Conf. Ser. 115.
- Mewe, R., Gronenschild, E.H.B.M., van den Oord, G.H.J., 1985. *A&AS*, 62, 197
- Mewe, R., Lemen, J.R., van den Oord, G.H.J., 1986. *A&AS*, 65, 511
- Mirabel, I.F., Sanders, D.B. & Kazes, I., 1989, *ApJ*, 340, L9
- Mushotzky, R.F & Szymkowiak, A.E., 1988, in *Cooling Flows in Clusters and Galaxies*, ed A.C. Fabian, Kluwer.
- Mushotzky, R.F., Loewenstein, M., Arnaud, K.A., Tamura, T., Fukazawa, Y., Matsushita, K., Kikuchi, K. & Hatsukade, I., 1996, *ApJ*, 466, 686
- O’Dea, C.P. & Baum, S.A., 1997, in *Galactic and Cluster Cooling Flows*, ed. N. Soker, ASP Conf. Ser. 115.
- Petre, R., Serlemitsos, P.J., Marshall, F.E., Jahoda, K. & Kunieda, H., 1992, *Proc. SPIE*, 1546, 72
- Raymond, J.C. & Smith, B.W., 1977, *ApJS*, 35, 419
- Sarazin, C.L., 1997, in *Galactic and Cluster Cooling Flows*, ed. N. Soker, ASP Conf. Ser. 115.
- Schattenburg, M.L., & Canizares, C.R., 1986, *ApJ*, 301, 759
- Serlemitsos, P.J., Marshall, F.E., Petre, R., Jahoda, K., Boldt, E.A., Holt, S.S., Mushotzky, R.F., Swank, J.H., Szymkowiak, A.E., Kelley, R. & Loewenstein, M., 1991, *Proceedings of 28th Yamada conference*, eds. Y. Tanaka & K. Koyama
- Stark, A.A., Gammie, C.F., Wilson, R.W., Bally, J., Linke, R.A., Heiles, C., Hurwitz, M., 1992, *ApJS*, 79, 77
- Verner, D.A., Ferland, G.J., Korista, K.T. & Yakovlev, D.G., 1996, *ApJ*, 465, 487
- Voit, G.M. & Donahue, M., 1993, *ApJ*, 414, L17
- Voit, G.M. & Donahue, M., 1995, *ApJ*, 452, 164
- Weaver, K.A., et al. , 1995, *ApJS*, 96, 303
- Woo, J.W., Forrey, R.C. & Cho, K., 1997, *ApJ*, 477, 235
- White, D.A., Fabian, A.C., Johnstone, R.M., Mushotzky, R.F., Arnaud, K.A., 1991. *MNRAS*, 252, 72

Table 1. Results of spectral fits

Model and Parameters	Fit values	(F94) ^a	χ^2/bins
Single temperature			1367/1043
Temperature	$4.22^{+0.07}_{-0.07}$ keV	(4.15)	
Abundance	$0.41^{+0.03}_{-0.03}$ of Solar	(0.48)	
Two temperature with absorption			1179/1043
Higher Temperature	$5.25^{+0.57}_{-0.33}$ keV	(5.62)	
Lower Temperature	$1.57^{+0.25}_{-0.21}$ keV	(2.05)	
Extra absorption	$0.22^{+0.12}_{-0.08} \times 10^{22} \text{cm}^{-2}$	(0.11)	
Abundance	$0.37^{+0.04}_{-0.03}$ of Solar	(0.39)	
Cooling flow (RS) with absorption			1211/1043
Temperature	$4.29^{+0.17}_{-0.15}$ keV	(4.21)	
Extra absorption	$0.29^{+0.04}_{-0.03} \times 10^{22} \text{cm}^{-2}$	(0.41)	
Abundance	$0.40^{+0.03}_{-0.03}$ of Solar	(0.46)	
Accretion rate	$180^{+26}_{-26} M_{\odot} \text{yr}^{-1}$	(138)	
Cooling flow (MK) with absorption			1211/1043
Temperature	$4.20^{+0.15}_{-0.14}$ keV	(4.20)	
Extra absorption	$0.35^{+0.06}_{-0.04} \times 10^{22} \text{cm}^{-2}$	(0.30)	
Abundance	$0.39^{+0.03}_{-0.04}$ of Solar	(0.43)	
Accretion rate	$154^{+23}_{-23} M_{\odot} \text{yr}^{-1}$	(122)	
Two temperature with O K-edge			1166/1043
Higher Temperature	$5.85^{+0.48}_{-0.68}$ keV		
Lower Temperature	$2.02^{+0.37}_{-0.44}$ keV		
Optical depth	$1.88^{+1.86}_{-0.56}$		
Abundance	$0.38^{+0.03}_{-0.04}$ of Solar		
Cooling flow (RS) with O K-edge			1185/1043
Temperature	$4.49^{+0.19}_{-0.16}$ keV		
Optical depth	$4.30^{+0.55}_{-0.46}$		
Abundance	$0.40^{+0.03}_{-0.04}$ of Solar		
Accretion rate	$180^{+23}_{-24} M_{\odot} \text{yr}^{-1}$		

^aAnalogous results from the ASCA SIS analysis by Fabian et al. (1994). The regions of the cluster from which spectra are accumulated are different for the ASCA SIS and BBXRT so these results are not precisely comparable. In particular, the measured mass accretion rates should differ.